SUPPLEMENTARY DATA

Supplementary Experimental procedures

RNA Isolation and PCR Analysis

Total RNA was isolated from liver tissue using Trizol® reagent (Invitrogen, Waltham, MA) and first-strand cDNA synthesis performed (2 μg total RNA) with SuperScript II (Invitrogen Waltham, MA,). PCR was performed using Eppendorf Realplex2 instrument with the gene specific primers listed below. All mRNA levels were normalized to cyclophilin (liver) or TBP (adipose) using a standard curve.

qPCR Primer Sequences

Name	Forward sequence	Reverse sequence
ACC	GGCGACTTACGTTCCTAG	AGGTGTCGATAAATGCGGTCC
FAS	TTCCGTCATTCCAGTTAGAGAG	TTCAGTGAGGCGTAGTAGACA
SCD	GTTGCCAGTTTCTTTCGTG	GGGAAGCCAAGTTTCTACACA
SRE	ATCCAAGGGCATCTGAGAACTC	GGCTATTCCGTGAACATCTCCTA
DGT1	GGATCTAGGTGCCATCGT	CCACCAGGATGCCATACTTG
DGT2	GGCTACGTTGGCTGGTAACTT	TTCAGGGTGACTGCGTTCTT
TGH	GGAGGGCAGGTGCTCTCA	GCCTTCAGCGAGTGGATAGC
CPT	TGAGTGGCGTCCTCTTTGG	CAGCGAGTAGCGCATAGTCATG
LCAD	GCGAAATACTGGGCATCTGAA	TCCGTGGAGTTGCACACATT
HMG	TGGGCATGAACATGATCTCTA	GGCTTCACAAACCACAGTC
LDLR	CCGTCTCTATTGGGTTGATT	GAGTCGATTGGCACTGAAA
G6PT	TTGCCTTGTTTGGAGTCATAG	CCCATCTTGGTGCGGATATT
GK	AATGTGAGGTCGGCATGATTGT	CCATGTACTTTCCGCCAATGAT
CYC	TCCAAAGACAGCAGAAAACTTTCG	TCTTCTTGCTGGTCTTGCCATTTCC
TFIIB	TGGAGATTTGTCCACCATGA	GAATTGCCAAACTCATCAAAACT
C/EBPα	TGGACAAGAACAGCAACGAG	TCACTGGTCAACTCCAGCAC
FABP4	TGGAAGCTTGTCTCCAGTGA	AATCCCCATTTACGCTGATG
TNFα	GTCTACTGAACTTCGGGGTGA	CACCACTTGGTGGTTTGCTACGAC
KLF4	GTCCTTCTCCACGTTCGC	CCAGGAGGTCGTTGAACTC
KLF5	GCCAACTCTCCCACCTGTCA	GTGCACTTGTAGGGCTTCTCG
PREF1	TGGCTTCTCAGGCAACTTCT	CTTGCACAGACACTCGAAGC
CD137	CGTGCAGAACTCCTGTGATAAC	GTCCACCTATGATGGAGAAGG
TBX1	GGCAGGCAGACGAATGTTC	TTGTCATCTACGGGCACAAAG
TMEM26	ACCCTGTCATCCCACAGAG	TGTTTGGTGGAGTCCTAAGGTC
UCP1	GGCCTCTACGACTCAGTACA	TAAGCCGGCTGAGATCTTGT
TCF21	CATTCACCCAGTCAACCTGA	TTCCTTCAGGTCATTCTCTGG
TBP	ACCCTTCACCAATGACTCCTATG	TGACTGCAGCAAATCGCTTGG

ACC, acetyl-CoA carboxylase; FAS, fatty acid synthase; SCD, stearoyl-CoA desaturase; SRE, sterol response element binding protein; DGT, diacylglycerol;acyl-CoA acyltransferase; TGH, triacylglycerol hydrolase, CPT, carnitine;palmitoyltransferase 1; LCAD, long chain acyl-CoA dehydrogenase; HMG, HMG-CoA reductase; LDLR, low-density-lipoprotein receptor; G6PT, glucose-6-phosphate transporter; GK, glucokinase; TFIIB, transcription factor IIB; C/EBP,

SUPPLEMENTARY DATA

CCAAT-enhancer-binding protein; FABP4, fatty acid binding protein 4; TNFα, tumor necrosis factor alpha; KLF, krupple-like factor; PREF1, Preadipocyte factor 1; TBX1, T-box transcription factor 1; TMEM26, transmembrane protein 26; UCP, uncoupling protein; TCF21, transcription factor 21.

SUPPLEMENTARY DATA

Supplementary Figure S1. Taz-deficiency decreases white adipose mass and liver steatosis while maintaining bone density and length. Unedited immunoblot image of dox-inducible knock-down of tafazzin protein in male transgenic (Tg) compared to non-transgenic (NTg) mice using isolated mitochondria from (**A**) heart (25 μg), skeletal muscle (50 μg) and liver (100 μg) liver) or (**B**) heart (12.5 μg), BAT (12.5 μg) and WAT (12.5 μg). Citrate synthase (cit) was used as a loading control (n=3-6). (**C**) Representative image of 10-month-old Tg and NTg mice fed a low-fat diet. (**D**) Bone mineral density (n=19-40) and (**E**) tibia length (n=7-14) were quantitated. Mass of perirenal white adipose tissue (**F**), brown adipose tissue (BAT) (**G**), liver (**H**) and (**I**) inguinal adipose tissue were expressed as a proportion of body weight (n=15-40). The mRNA levels of the indicated genes measured in inguinal (**J**) and gonadal (**K**) adipose tissue by qPCR (n=2-8). (**L**) Hepatic microvesicular steatosis was quantified (n=5-7). Data are expressed means ± SEM (* $P<0.05$, compared to NTg age-matched mice fed the identical diet, † $P<0.05$, Tg +dox compared to all other groups, ‡ $P<0.05$ NTg +dox compared to all other groups).

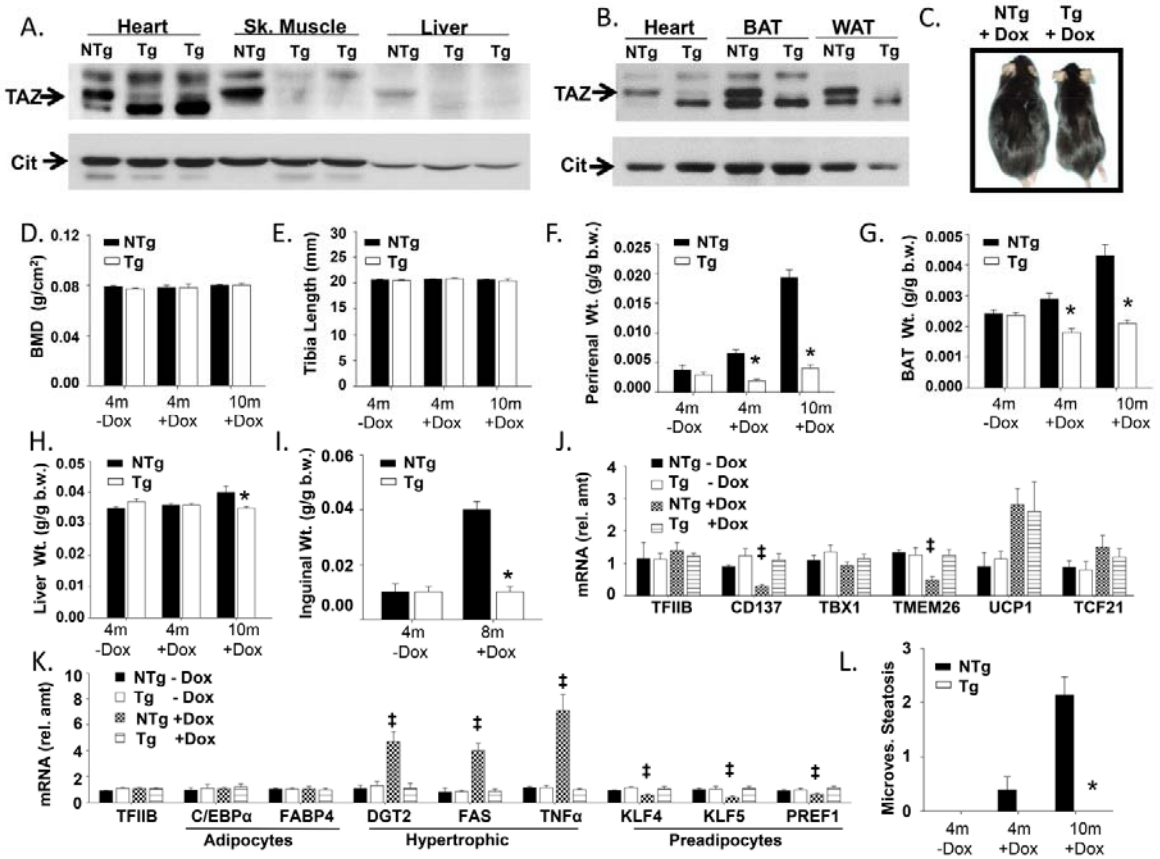

SUPPLEMENTARY DATA

Supplementary Figure S2. Taz-deficiency reduces white adipose, liver steatosis and plasma hypercholesterolemia following 16 weeks of a high-fat diet. (**A**) The mass of various fat pads expressed per body weight (b.w.) (n=15-16). (**B**) Hepatic macrovesicular and microvesicular steatosis scores (n=8). (**C**) Plasma alanine aminotransferase (ALT), (**D**) plasma non-esterified fatty acids (NEFA), (**E**) plasma lipid levels and (**F-G**) plasma lipoproteins from fasted animals were separated by FPLC into very-low-density (VLDL), low-density (LDL) and high-density (HDL) lipoproteins. TG and total cholesterol (Chol, unesterified + esterified) were measured in each FPLC fraction. Each curve represents mean values from 3-5 mice. Food (**H**) and water (**I**) consumption were measured in Tg and NTg mice after 3 or 16 weeks of a high-fat diet and expressed as a proportion of body weight (b.w.) (n = 6-10). BAT, brown adipose tissue. Data are expressed as means ± SEM (* P<0.05, compared to NTg age-matched mice fed the identical diet).

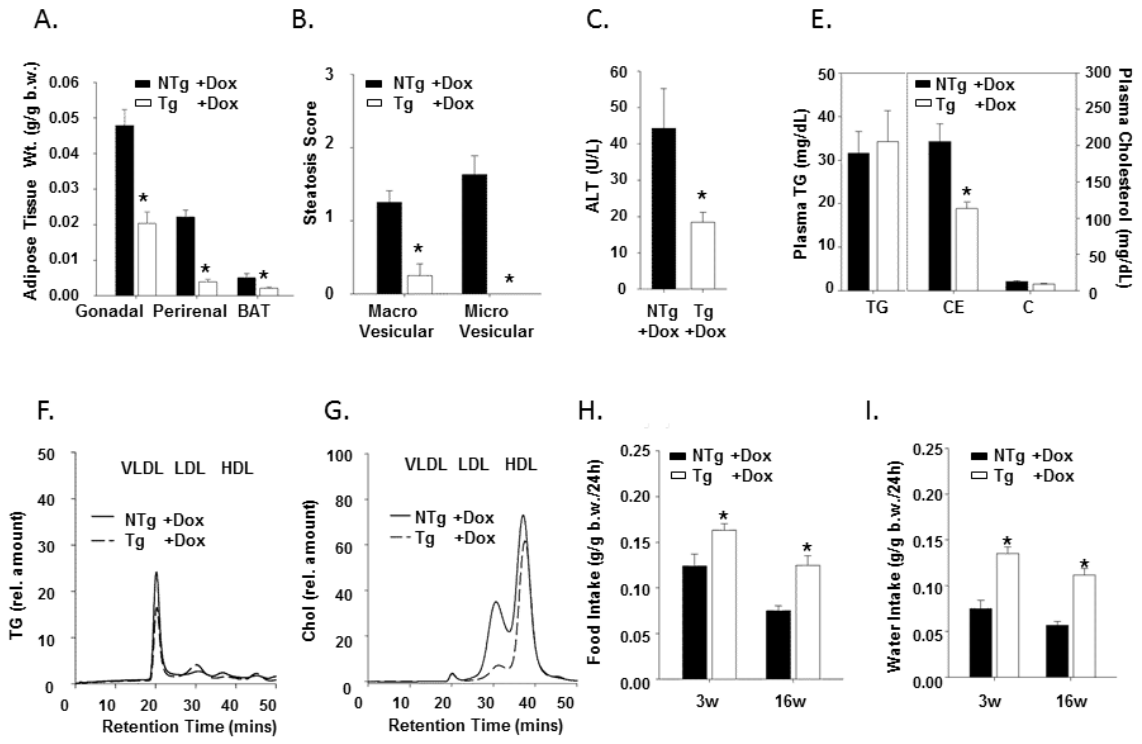

SUPPLEMENTARY DATA

Supplementary Figure S3. The amount of mitochondrial complex protein and supercomplex formation are unaltered in the liver by Taz-deficiency. Immunoblot of mitochondrial complexes I-V in heart (**A**), skeletal muscle (soleus) (**D**) and liver (**H**) whole lysates (20 μg protein). Unedited images of mitochondrial supercomplexes visualized by in-gel activity assays for mitochondrial complexes I (**B, E, I**), and IV (**C, F, J**) (heart, skeletal muscle & liver respectively). The location of each individual complex is indicated as CI, or CIV respectively. The supercomplexes which contain the complex of interest (i.e. active complex) are indicated with brackets at the top of each gel. The size of the ladder is indicated in kDa on the left.

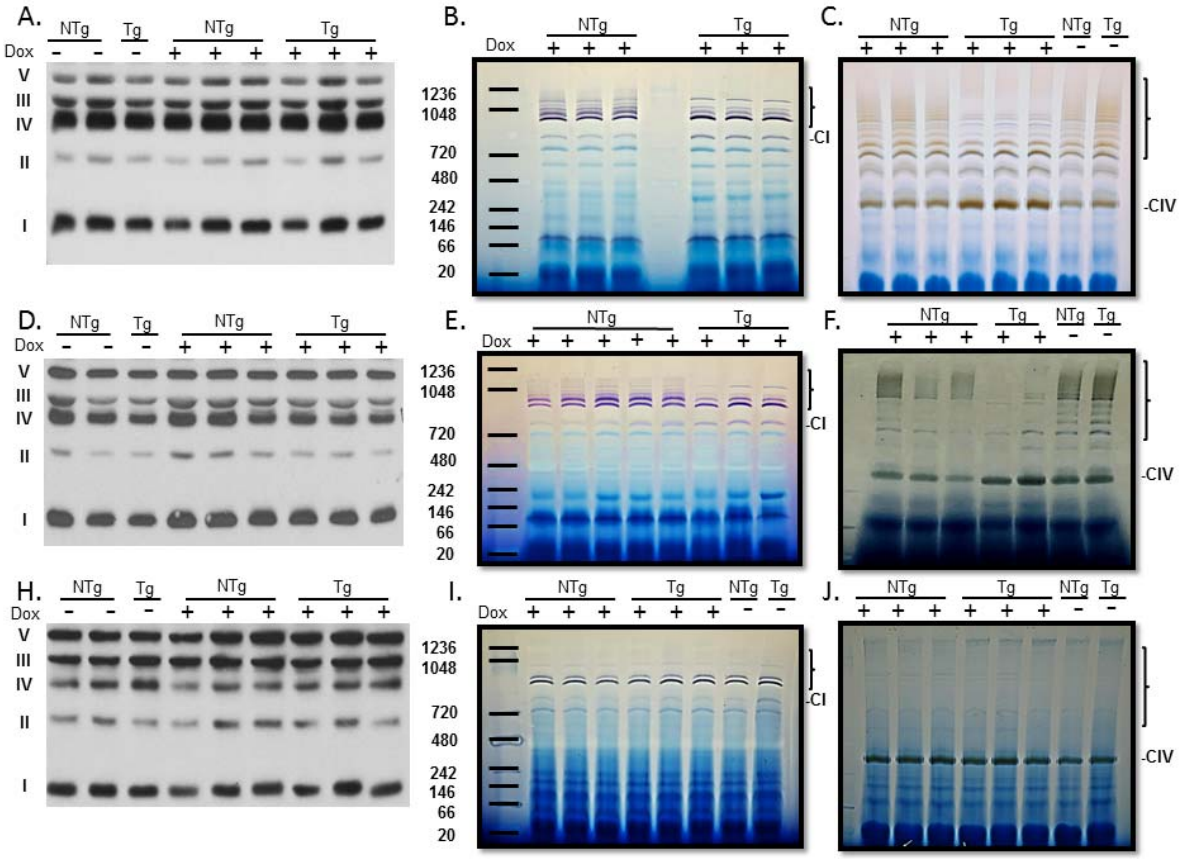

SUPPLEMENTARY DATA

Supplementary Figure S4. The assessment of cardiolipin content and supercomplex formation in various adipose tissues. The molecular species of CL in BAT (**A**) was determined by MS/MS and arranged by mass with total cardiolipin content shown in the inset (n=6-7). The total cardiolipin content of WAT was determined in whole lysates (**B**) (n=4-6) and isolated mitochondria (**C**) (n=1-4). Immunoblot of mitochondrial complexes I-V in BAT (**D**), and gonadal white adipose tissue (**G**) whole lysates (50 µg protein BAT, 100 µg protein WAT). Images of mitochondrial supercomplexes visualized by in-gel activity assays for mitochondrial complexes I (**E, H**), and IV (**F, I**) (BAT & WAT respectively). The location of each individual complex is indicated as CI, or CIV respectively. The supercomplexes which contain the complex of interest (i.e. active complex) are indicated with brackets at the top of each gel. The size of the ladder is indicated in kDa on the left. Data are expressed means ± SEM (* $P<0.05$, compared to NTg age-matched mice fed the identical diet, † $P<0.05$, Tg +dox compared to all other groups).

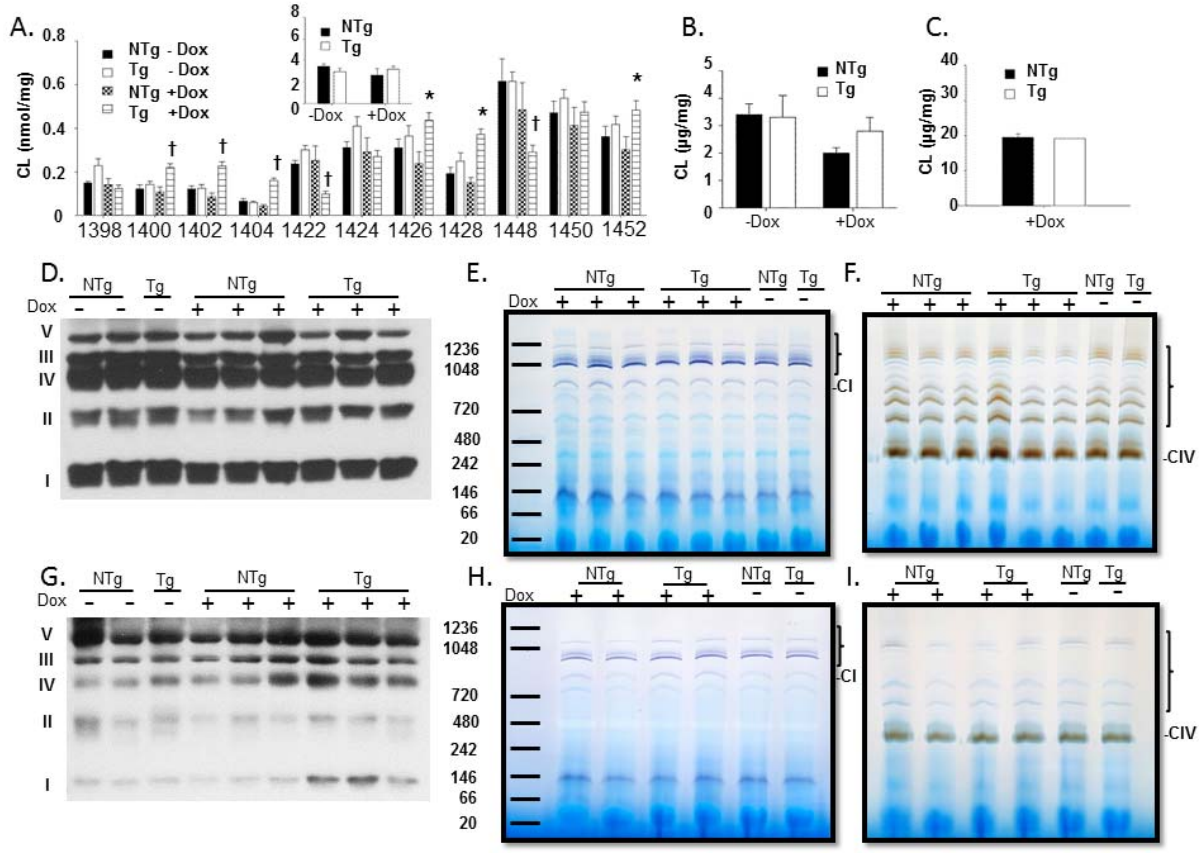

SUPPLEMENTARY DATA

Supplementary Figure S5. Mitochondrial oxidation of fatty acids is reduced in skeletal muscle from Taz-deficient mice. (**A-C**) Primary cultures of skeletal muscle fibers from the flexor digitorium brevis were isolated, cultured in 25 mM glucose and basal respiratory (**A**), ATP-sensitive (oligomycin sensitive)(**B**), ATP-insensitive (i.e. heat) (**C**), and maximum (FCCP) (**D**), oxygen consumption rates measured and expressed per mg of cellular protein (n = 6). (**E-H**) Primary skeletal muscle fibers from the flexor digitorium brevis were isolated, cultured in 0.175 mM Palmitate-BSA in the presence of 40 μM etomoxir or vehicle (water) and basal respiratory (**E**), ATP- sensitive (**F**), ATP-insensitive (**G**) and maximum (**H**) oxygen consumption was measured (n = 6). Fatty acid dependent respiration is the difference in oxygen consumption measured in the presence and absence 40 μM etomoxir. Values are means ± SEM (* P<0.05, compared to NTg age-matched mice fed the identical diet).

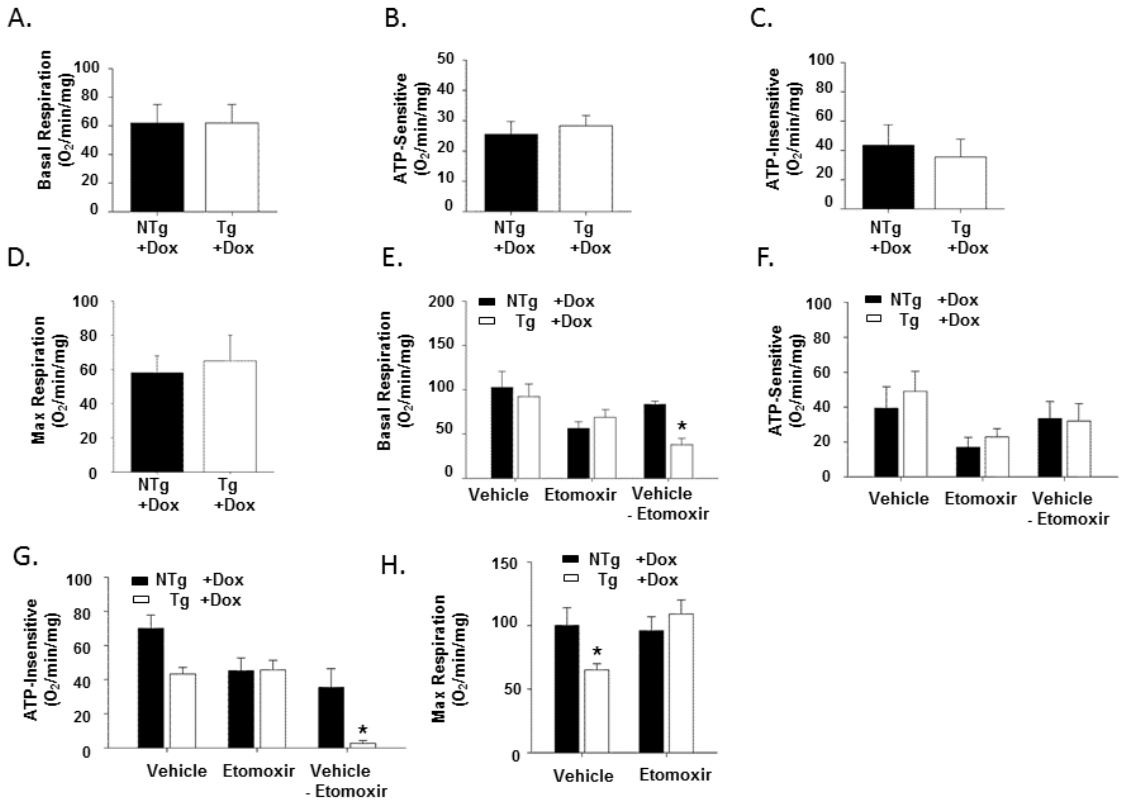

SUPPLEMENTARY DATA

Supplementary Figure S6. Analysis of lipid metabolism in various tissues. (**A**) The accumulation of newly secreted hepatic TG in the plasma of fasted (16 h) 4-month-old mice following i.p. injection with Poloxamer 407 (n=3-9). (**B**) Hepatocytes were incubated with [^{14}C]-oleate, media collected at the indicated times and radiolabel in secreted TG measured. (**C-D**) Hepatocytes were incubated with [^{14}C]-oleate (**C**) or [^{14}C] acetate (**D**) for the times indicated and the incorporation of radiolabel into PC measured (n=4-7). Immunoblot of MTPa, UCPs and loading control (tubulin) in skeletal (**E**), heart (**F**), BAT (**G**) and WAT (**I**) total cell lysates (20 µg protein skeletal & heart, 50 µg protein BAT, 100 µg protein WAT). (**H**) Plasma levels of non-esterified fatty acids in fasted high-fat fed mice (n=15-16). Quantitation of ATGL (**J**) and P-HSL (Ser 660) (**K**) immunoblots by densitometry with normalization against tubulin or total HSL (n=4-6). Plasma levels of adrenaline (**L**) and noradrenaline (**M**) were quantified (n=2-10). Values are means ± SEM. (* P<0.05, compared to NTg age-matched mice fed the identical diet, ‡ P<0.05, NTg +dox compared to all other groups).